A Model for Educational Simulation of Infant Cardiovascular Physiology

Jane A. Goodwin, MD*†, Willem L. van Meurs, PhD*‡§, Carla D. Sá Couto, MSc§, Jan E. W. Beneken, PhD*, and Shirley A. Graves, MD*

*Department of Anesthesiology, University of Florida College of Medicine, Gainesville, Florida; †Nemours Children's Clinic-Jacksonville, Jacksonville, Florida, and Mayo Medical School, Rochester, Minnesota; ‡Medical Education Technologies, Inc., Sarasota, Florida; and §Instituto de Engenharia Biomédica, Laboratório de Sinal e Imagem Biomédica, Porto, Portugal

Full-body patient simulators provide the technology and the environment necessary for excellent clinical education while eliminating risk to the patient. The extension of simulator-based training into management of basic and critical situations in complex patient populations is natural. We describe the derivation of an infant cardiovascular model through the redefinition of a complete set of parameters for an existing adult model. Specifically, we document a stepwise parameter estimation process, explicit simplifying assumptions, and sources for these parameters. The simulated vital signs are within the target hemodynamic variables, and the simulated systemic arterial pressure wave form and left ventricular pressure volume loop are realistic. The system reacts appropriately to blood loss, and incorporation of aortic stenosis is straightforward. This infant cardiovascular model can form the basis for screen-based educational simulations. The model is also an essential step in attaining a full-body, model-driven infant simulator.

(Anesth Analg 2004;99:1655–64)

Traditional medical education relies on the clinical setting to teach students, residents, and other medical personnel. However, this is not an ideal learning environment because the learning experience may be limited by the critical condition of the patient. Full-body patient simulators provide the technology and the environment necessary for excellent clinical education while eliminating risk to the patient. Currently, more than 450 full-body model-driven simulators are being used throughout the world to teach basic skills (1), responses to complex problems (2), and crisis resource management (3) to a variety of personnel, including residents, medical students, and allied health care professionals.

The extension of simulator-based training into management of basic and critical situations in complex patient populations is natural. Complex models have been adapted to simulate the cardiovascular physiology of the obstetric patient (4). A simulation-based training program in neonatal resuscitation has also been developed (5). Obstetric patients, neonates, and children often present a management challenge in the acute care setting because of complex physiology and the need for swift therapeutic interventions. The modeling of pediatric cardiovascular physiology is an important step in attaining a full-body model-driven pediatric simulator that can be used for clinical education. The cardiovascular physiology of the neonate, infant, child, and adolescent all differ because of continuing development and maturation of the cardiovascular system. Although each pediatric patient may present a unique challenge to the acute care provider, we based the cardiovascular physiology of our simulated patient on that of an infant.

The cardiovascular system of an infant differs significantly from that of an adult, and, therefore, modeling the cardiovascular physiology requires the redefinition of a complete set of parameters. Our hypothesis was that the described model structure could adequately reflect pediatric cardiovascular physiology for educational simulation purposes. Our goal was to find model parameters such that the cardiovascular vital signs reflect target pediatric vital signs in normal and pathologic conditions and that they react appropriately to critical incidents and

Funded by the Department of Anesthesiology, University of Florida College of Medicine, Gainesville, FL, and Medical Educational Technologies, Inc., Sarasota, FL.

Accepted for publication May 18, 2004.

Address correspondence to Jane A. Goodwin, MD, Nemours Children's Clinic-Jacksonville, 807 Children's Way, Jacksonville, FL 32207. Address e-mail to jgoodwin@nemours.org. Reprints will not be available from the authors.

DOI: 10.1213/01.ANE.0000134797.52793.AF

0003-2999/04

therapeutic interventions. The selected basic critical incident was moderate acute blood loss. To evaluate the capacity of our model to reflect pathology, we chose aortic stenosis.

Methods

In our study, we used the linearized, improved model of cardiovascular physiology presented by Beneken (6) (Fig. 1) to represent the uncontrolled cardiovascular system. This model was also the basis for the model of cardiovascular physiology for the Human Patient Simulator (HPS™; developed at the University of Florida and commercially available from Medical Education Technologies, Inc., Sarasota, FL). This uncontrolled model was selected because although it is of relatively reduced complexity, it could support a wide range of anticipated learning objectives. The model can generate pulsatile blood pressure wave forms and reacts appropriately to blood loss and volume administration, intrathoracic pressure, baroreflex control of circulation, and drug influences.

A physiologic interpretation of the model structure and parameter values is desirable for easy coupling of this model to other models and for adjustment of parameter values to reflect pathologies, critical incidents, or other patients. The interactive simulation application requires the model to run in real time. The 1965 model was used because some of the added detail in the later models (7) or in the HPS implementation was judged unnecessary for the present application. In our study, we used the baroreflex model presented by Wesseling and Settels (8). Appendix 1 describes these models in detail. The interfacing of model input and output signals to the simulator mannequin and the monitors, as well as the interactions of the cardiovascular model with other physiologic models, is described elsewhere (9).

Adapting the above-described model to simulate the cardiovascular system of a pediatric patient involved several steps. First, target hemodynamic variables for the patient—specifically, a 6-mo-old infant—were defined by reviewing pediatric and pediatric anesthesia textbooks (10,11) and are listed together with the simulation results in Table 1 (second column). To further simplify the development process, we observed that opening the cardiovascular loop would allow us to work on the left/systemic and right/pulmonary sides of the cardiovascular system independently. The second step consisted of temporarily fixing the model parameters: pulmonary venous pressure to 4 mm Hg and intrathoracic systemic venous pressure to 3 mm Hg. This created a system that allowed independent manipulation of left heart and systemic vascular parameters and of right heart and pulmonary vascular parameters. In this phase, physiologic model parameters were derived from the literature and incorporated into the model. Once target values were achieved for each uncontrolled system half independently, the third step consisted of lifting the restrictions on the pulmonary and systemic venous pressure and combining the two systems to yield a full uncontrolled system. In the last step, the influence of the baroreflex was added, governing the system behavior when it receives a perturbation. The dynamic response to blood loss is evaluated in this controlled system. As a test of the capability of this model to reflect pathologies via the adjustment of model parameters, we obtained data for aortic valve stenosis and simulated this pathology.

Review of published literature provided clinical variables that describe the left ventricular function and global descriptions of the systemic and pulmonary circulation of an approximately 6-mo-old infant (Table 2). However, cardiovascular data for the healthy infant were not as plentiful as for the healthy adult. In addition, one cannot assume that animal data always correlate well with that for humans. With these facts in mind, certain model parameters were obtained directly from the literature, some were derived through the use of well established formulas, and still others required that physiologically sound assumptions be made. We have explicitly documented these steps. Appendix 2 describes the parameter-estimation procedure and its assumptions.

The model simulation results that were validated first were normal heart rate, cardiac output, and systemic arterial, central venous, pulmonary arterial, and pulmonary capillary wedge pressures. We also showed the generated pulsatile arterial blood pressure wave form. We further presented simulation results on the model response to acute moderate blood loss and validated the simulated vital signs for aortic stenosis.

Congenital aortic stenosis may be caused by a spectrum of lesions that obstruct blood flow from the left ventricle to the aorta. Inclusion in an educational simulation is relevant for the training in recognition of and possible therapeutic interventions on an infant with this condition. Three parameter changes were made to the model. The aortic valve and intrathoracic artery resistance (Appendix 2) was increased from 0.016 to 0.8 mm $Hg \cdot mL^{-1} \cdot s$. On the basis of a left ventricular pressure volume curve given by Graham and Jarmakani (12), we changed the left ventricular filling characteristics by increasing the diastolic elastance of the left ventricle from 0.55 to 1.5 mm Hg/mL while reducing the unstressed volume from 2 to 0 mL. This is thought to reflect the reduced compliance and unstressed volume due to the increased cardiac muscle mass.

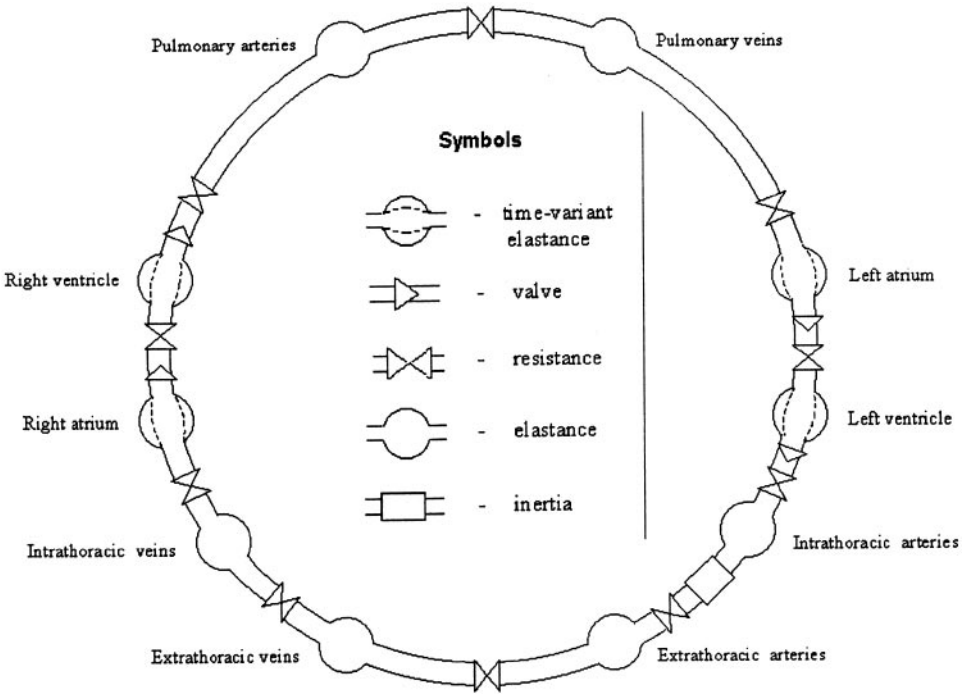

Figure 1. Hydraulic analog for the cardiovascular model.

Table 1. Simulated Cardiovascular Vital Signs for a 6-Month-Old Infant

		Simulation results					
		Independent systems			Full circulation		
Variable	Target	Left/ systemic	Right/ pulmonary	Right/ pulmonary (2)	Baseline	50-mL Blood loss	Aortic stenosis
Heart rate (bpm)	115–145	129	129	129	129	135	140
Systemic systolic pressure (mm Hg)	70–110	89			86	82	76
Systemic diastolic pressure (mm Hg)	50–65	59			57	56	57
Central venous pressure (mm Hg)	3–12	3	3	3	3	2	3
Pulmonary systolic pressure (mm Hg)	12–28		21	16	16	14	20
Pulmonary diastolic pressure (mm Hg)	4–12		7	6	6	5	12
Pulmonary capillary wedge pressure (mm Hg)	NA	4	4	4	4	3	10
Cardiac output (L/min)	1.2–2.0	1.8	2.6	1.8	1.8	1.6	1.5

NA = not available.
The second iteration for the right/pulmonary side and full circulation uses a reduced right heart contractility.

The model equations were numerically integrated by using the Euler forward method with a step size of 1 ms. All simulations were implemented in Microsoft Visual Java++ Version 6.0 on a personal computer with an 1800-MHz Pentium™ 4 processor.

Results

Table 1 gives the target values and simulated vital signs. When the isolated halves were simulated (Appendix 2), the vital signs for the left/systemic side were within the target values. The pressures for the right/pulmonary side were within the target values, but the cardiac output was high. Moreover, it was higher than the cardiac output of the isolated left/systemic side. The contractility of the right ventricle, as reflected in the ERVMAX (maximum systolic elastance of the right ventricle) parameter, was not directly derived from a measured pressure-volume loop, but rather through scaling from the left ventricle. We therefore adjusted this parameter and the corresponding right atrial parameter ERAMAX (maximum systolic elastance of the right atrium) to obtain a similar cardiac output for the right/pulmonary part of the circulation. A reduction of 40% was necessary. This second iteration is also reflected in Table 1. The "Baseline" column of this table demonstrates that combining the isolated halves into the full circulation did not significantly influence the simulated vital signs and

Table 2. Clinical Variables Describing Left Ventricular Function and Global Descriptions of the Systemic and Pulmonary Circulation of an Approximately 6-Month-Old Infant from the Literature (Assumed Body-Surface Area, 0.4 m^2)

Variable	Absolute value	Normalized value	Reference
Heart			
LVEDV	17 mL	42 mL/m^2	12
LVEDP	5 mm Hg		12
LVESV	5 mL	13 mL/m^2	12
LVESP	82 mm Hg		12
Circulation			
SVR	25–50 mm Hg · L^{-1} · min	10–20 mm Hg · L^{-1} · min · m^2	17
PVR	2.5–7.5 mm Hg · L^{-1} · min	1–3 mm Hg · L^{-1} · min · m^2	17
Arterial compliance	0.46 mL/mm Hg	1.15 mL · mm Hg^{-1} · m^{-2}	19

LVEDV = left ventricular end-diastolic volume; LVEDP = left ventricular end-diastolic pressure; LVESV = left ventricular end-systolic volume; LVESP = left ventricular end-systolic pressure; SVR = systemic vascular resistance; PVR = pulmonary vascular resistance.

that they were well within the ranges of the target vital signs. Results from the echocardiographic study of 30 infants performed by Wodey et al. (13) provided data for baseline heart rate, systolic blood pressure, cardiac index, and shortening fraction. Their results further substantiate the clinical appropriateness of our simulated vital signs. In this simulation experiment, we used a total blood volume of 685 mL, which is slightly more than the approximately 640 mL expected for an 8-kg infant.

The pulsatile nature of the model is highlighted by the simulation results in Figures 2 and 3. Figure 2 shows the systemic arterial blood pressure wave form. We consider this wave form realistic enough for the envisioned simulation application in acute care training. Figure 3 (normal case) shows the simulated left ventricular pressure-volume loop and the clinical variables and the assumed value for the unstressed volume from which the left ventricle model parameters were calculated. The curve, simulated with a full circulation model, reproduces the clinical variables characterizing the end-diastolic and end-systolic situations in good approximation.

For our 6-mo-old infant, an acute blood loss of 50 mL corresponds to an approximately 7% loss in blood volume. The simulated vital signs demonstrate an appropriate clinical response (Table 1; "50-mL Blood loss" column). Note that the "Baseline" column in Table 1 represents the vital signs of the system with baroreflex control in its baseline operating point. These vital signs are identical, by design, to the vital signs of the uncontrolled full circulation.

Figure 3 also shows the simulated left ventricular pressure-volume loops with aortic stenosis. The changes are indeed very similar to the ones reported by Graham and Jarmakani (12). Table 1 (final column) lists the effects on the monitored signals. From Figure 3 and the systemic systolic pressure in Table 1 we observed that the pressure difference across the stenotic valve was approximately 90 mm Hg, corresponding to a severe stenotic situation. From the same figure and table, we note that for the simulated normal infant, there is no apparent stenotic pressure decrease. With the indicated integration step size, programming language, and hardware, the cardiovascular model runs 300 times faster than real time.

Discussion

From the perspective of educational simulations of clinical scenarios, the main differences between the cardiovascular system of an infant and an adult are quantitative rather than qualitative. Therefore, modeling the cardiovascular physiology in this context does not require formulating a new model structure, but it does require the redefinition of a complete set of parameters. We describe an existing simulation model and the derivation of a new parameter set for the infant cardiovascular system. Several parameters were derived through proportionality constants or adjustments. The simulated vital signs were within the target hemodynamic variables, and the system reacts appropriately to blood loss. Arterial pressure wave forms and left ventricular pressure volume curves were, in our opinion, realistic enough for educational simulations. From the simulation of aortic stenosis, we concluded that through only a few simple and intuitive parameter changes, we can manipulate our model to realistically reflect essential aspects of aortic stenosis.

A simulation engine of a medical simulator typically includes many other models, and other simulator functionality requires further processing time. Our simulation results show that run time is not a limiting factor to the complexity of this model. However, increasing model complexity would further complicate the already extensive parameter-estimation procedure and make future manipulation by clinical instructors to simulate other patients, pathologies, and incidents virtually impossible.

Two fundamental physiologic aspects complicate both teaching and parameter estimation of the cardiovascular system. The first aspect is the circular nature of the system. A change in any part of the circulation will

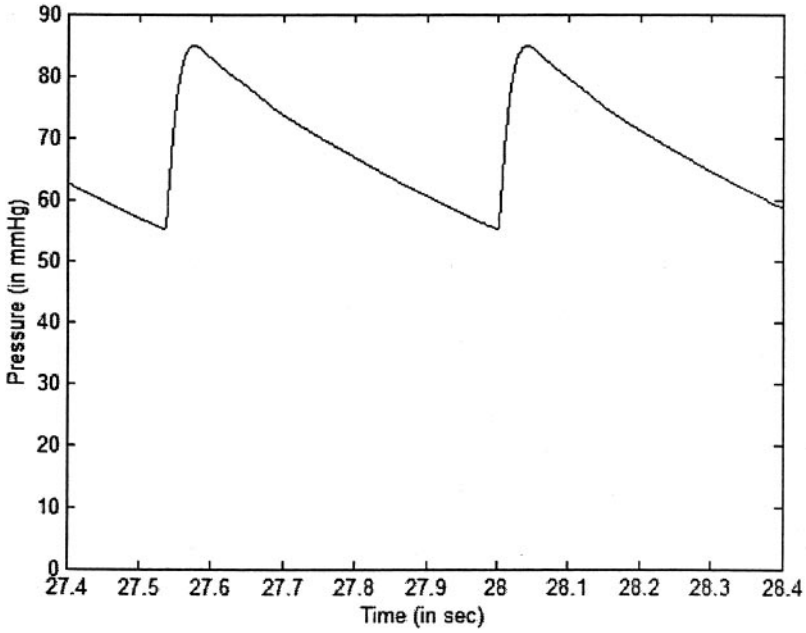

Figure 2. Simulated systemic arterial blood pressure.

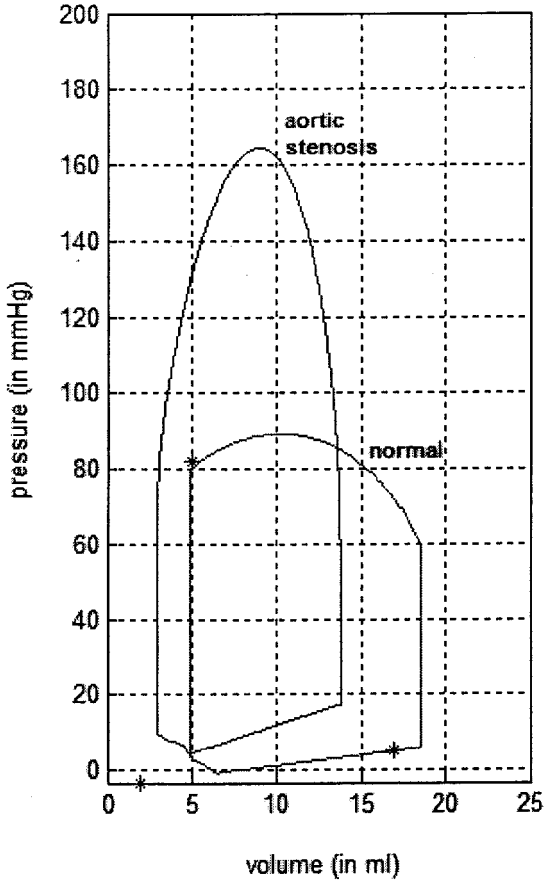

Figure 3. Simulated left ventricular pressure-volume loops with and without aortic stenosis. *Clinical variables and the assumed unstressed volume from which the model parameters were derived.

affect blood volumes, pressures, and flow rates in all parts. The second aspect is control by the baroreflex. This powerful control system also spreads out the effect of a local change to many parts of the circulation and masks the dependency of system variables on system parameters. We solved both problems by initially considering the left/systemic and right/pulmonary sides of the uncontrolled cardiovascular system independently. The ability to work on a smaller set of parameters, and without the circular effect of a parameter change, did facilitate identifying and adjusting a problem with the contractility of the right heart. After combining the two sides of the circulation, we then incorporated a model of basic aspects of the baroreflex.

This model can form the basis for a screen-based teaching tool. The model may be used to demonstrate the many clinically important differences between normal infant and adult cardiovascular physiology. Clinical scenarios may be created to demonstrate specific learning objectives. In addition, this model may be used as the underlying model for the uptake and distribution of respiratory and anesthetic gases, as well as simulation of the effects of anesthetics. Models for the simulation of the myocardial oxygen balance and electrophysiologic phenomena can easily be coupled to it, with the ultimate goal of simulation of a six-month-old infant in full scale.

Appendix 1: A Model for Adult Cardiovascular Physiology

The uncontrolled cardiovascular model (Figure 1) accepts as inputs blood volume changes and intrathoracic pressure and generates as outputs systemic and

pulmonary artery blood pressures, central venous and all pulmonary artery catheter blood pressures, and cardiac output. Note that in the 1965 model, the pressure decreases over the systemic and pulmonary beds are represented by a single resistance each; this model does not represent the accumulation of blood in tissue, nor does it reflect distinct parallel vascular beds.

For each model compartment, the variables blood pressure, inflow rate, and volume change are computed. The compartment equations are coupled because the inflow rate of a compartment also depends on the pressure of the upstream compartment, and the volume change results from the difference between inflow and outflow rates. The relationships between variables are governed by resistance, elastance, and unstressed volume. The elastances of the heart chambers vary and reflect the contraction. Transmural compartment pressure [p(t)] is a linear function of the difference between the compartment volume [v(t)] and the unstressed volume (UV) (for v(t) > UV). For selected compartments, average intrathoracic pressure is added to the transmural pressure to obtain the absolute pressure. The elastance (E) is the second parameter in the volume-pressure relationship:

$$p(\mathrm{t}) = E(v(\mathrm{t}) - \mathrm{UV}) \tag{A1}$$

The elastances of the heart chambers are time varying, reflecting the contraction. Compartment inflow rate [f(t)] is a linear function of the pressure in the upstream compartment [p_{in}(t) and p(t)]. The inflow resistance (R) governs this relationship:

$$f(\mathrm{t}) = \frac{p_{\mathrm{in}}(\mathrm{t}) - p(\mathrm{t})}{R} \tag{A2}$$

The resistances of the atrial inflow tracts to backward flow are 10 times superior to the resistances to forward flow. The resistances of the heart valves are also nonlinear, reflecting the infinite cardiac valve resistance to back flow. The change of compartment volume is equal to the difference between f(t) and the compartment outflow rate [f_{out}(t)]:

$$\frac{dv(\mathrm{t})}{dt} = f(\mathrm{t}) - f_{\mathrm{out}}(\mathrm{t}) \tag{A3}$$

A single differential equation governs the inertial behavior of the blood in the arteries by using a similar notation as in Table 3, formally introduced in Appendix 2:

$$\frac{df_{\mathrm{etha}}(\mathrm{t})}{dt} = \frac{p_{\mathrm{itha}}(\mathrm{t}) + \mathrm{PTH} - \mathrm{RETHA}\, f_{\mathrm{etha}}(\mathrm{t}) - p_{\mathrm{etha}}(\mathrm{t})}{\mathrm{LETHA}} \tag{A4}$$

Beneken (6) derived the parameter values that represent a normal adult in the supine position for the uncontrolled model from a combination of clinical data and computation based on physics (Table 3).

The description of the heart is critical for the estimation of the infant parameters and will be given in detail. Figure 4A shows a typical ventricular pressure-volume loop and the clinical variables that are used to characterize it. Such a loop can be generated by a time-varying elastance model of the ventricle (7):

$$p(\mathrm{t}) = e(\mathrm{t})[v(\mathrm{t}) - \mathrm{UV}], \tag{A5}$$

where p(t) is the ventricular pressure and v(t) the ventricular volume as a function of time. The relationship between these variables is determined by the unstressed volume (UV) and the elastance time profile [e(t)]. Suga et al. (14) verified this model in dogs and showed that e(t), which is characterized by its maximum value and the time of this maximum, reflects the ventricular contractility. We parameterized the ventricular elastance curve as follows:

$$e(\mathrm{t}) = \begin{cases} EMIN + (\mathrm{EMAX} - EMIN)\dfrac{t - (T_{\mathrm{as}} + T_{\mathrm{av}})}{K_{\mathrm{n}} T_{\mathrm{vs}}} \sin\left(\pi \dfrac{t - (T_{\mathrm{as}} + T_{\mathrm{av}})}{T_{\mathrm{vs}}}\right) \\ \qquad if\ (T_{\mathrm{as}} + T_{\mathrm{av}} \le t < T_{\mathrm{as}} + T_{\mathrm{av}} + T_{\mathrm{vs}}) \\ EMIN \quad (otherwise) \end{cases} \tag{A6}$$

The minimum and maximum elastances are EMIN and EMAX, respectively. T_{as}, T_{av}, and T_{vs} are the durations of atrial systole, atrioventricular delay, and ventricular systole, respectively. K_{n} is a normalization constant equal to the maximum of the time function

$$\{[t - (T_{\mathrm{as}} + T_{\mathrm{av}})]/T_{\mathrm{vs}}\} \sin\{\pi[t - (T_{\mathrm{as}} + T_{\mathrm{av}})]/T_{\mathrm{vs}}\},$$

part of Equation A6. It can be observed that this curve is a reasonable approximation of the curve for the left ventricle calculated from measured data by Suga et al. (14). Figure 4B shows the same pressure-volume loop as in Figure 4A, now with the model parameters UV, EMIN, and EMAX. This figure also shows a second curve that is obtained under different preload conditions, but with the same model parameters. The model parameters can be derived directly when a number of measured curves are available. If only clinical descriptors, such as in Figure 4A, are available, and provided that we have an estimate for the unstressed volume UV, EMIN and EMAX can be calculated as follows:

$$\mathrm{EMIN} = \frac{\mathrm{EDP} - \mathrm{PTH}}{\mathrm{EDV} - \mathrm{UV}} \tag{A7}$$

Table 3. Cardiovascular Parameters for the Adult and Infant

Part of circulation	Compartment	Parameter description	Parameter name	Parameter values	
				Adult	Infant
Total circulation		Initial total blood volume	VTOTAL	4740	685
Heart	Atria and ventricles	Heart rate	HR	72	129
Intrathoracic	All intrathoracic	Average intrathoracic pressure	PTH	−4.0	−3.25
Left heart	Left atrium	Resistance to forward flow of the inflow tract	RLAIN	0.00300	0.006
		Mitral valve resistance	RLAOUT	0.00300	0.006
		Diastolic elastance	ELAMIN	0.120	0.733
		Maximum systolic elastance	ELAMAX	0.280	1.99
		Unstressed volume	VLAU	30.0	1.00
	Left ventricle	Aortic valve and intrathoracic artery resistance	RLV	0.00800	0.016
		Diastolic elastance	ELVMIN	0.0900	0.550
		Maximum systolic elastance	ELVMAX	4.00	28.4
		Unstressed volume	VLVU	60.0	2.00
Systemic circulation	Intrathoracic arteries	Elastance	EITHA	1.43	7.76
		Unstressed volume	VITHAU	140	18.2
	Extrathoracic arteries	Blood flow inertia	LETHA	0.000700	0.000200
		Resistance	RETHA	0.0600	0.120
		Elastance	EETHA	0.556	3.02
		Unstressed volume	VETHAU	370	48.1
	Systemic peripheral vessels	Resistance	RSP	1.00	2.00
	Extrathoracic veins	Resistance (to forward flow)	RETHV	0.0900	0.180
		Elastance	EETHV	0.0169	0.0918
		Unstressed volume	VETHVU	1000	130
	Intrathoracic veins	Elastance	EITHV	0.0182	0.0989
		Unstressed volume	VITHVU	1190	155
Right heart	Right atrium	Resistance to forward flow of the inflow tract	RRAIN	0.00300	0.00600
		Tricuspid valve resistance	RRAOUT	0.00300	0.00600
		Diastolic elastance	ERAMIN	0.0500	0.317
		Maximum systolic elastance	ERAMAX	0.150	0.63
		Unstressed volume	VRAU	30.0	1.5
	Right ventricle	Pulmonic valve and pulmonary artery resistance	RRV	0.00300	0.00600
		Diastolic elastance	ERVMIN	0.0570	0.348
		Maximum systolic elastance	ERVMAX	0.490	2.09
		Unstressed volume	VRVU	40.0	3.0
Pulmonary circulation	Pulmonary arteries	Elastance	EPA	0.233	1.27
		Unstressed volume	VPAU	50.0	6.50
	Pulmonary peripheral vessels	Resistance	RPP	0.110	0.220
	Pulmonary veins	Elastance	EPV	0.0455	0.247
		Unstressed volume	VPVU	350	45.5

Units are as follows: heart rates, bpm; resistances, mm Hg · mL^{-1} · s; elastances, mm Hg/mL; volumes, mL; inertia, mm Hg · mL^{-1} · s^2.

$$\mathrm{EMAX} = \frac{\mathrm{ESP} - \mathrm{PTH}}{\mathrm{ESV} - \mathrm{UV}} \qquad \text{(A8)}$$

Note that in the calculation of these slopes, we use the (average) intrathoracic pressure (PTH) as a reference, rather than 0 (atmospheric pressure). This can be made plausible by observing that the unstressed volume occurs at a zero transmural pressure across the ventricular wall, which requires a ventricular pressure equal to the intrathoracic pressure. The atrial elastance curves are identical to those proposed by Beneken (6) and are parameterized as follows:

$$e(t) = \begin{cases} \mathrm{EMIN} + (\mathrm{EMAX} - \mathrm{EMIN}) \sin\left(\pi \frac{t}{T_{as}}\right) & (0 \le t < T_{as}) \\ \mathrm{EMIN\ (otherwise)} \end{cases} \qquad \text{(A9)}$$

The minimum and maximum elastances are EMIN and EMAX, respectively, and T_{as} is the duration of the

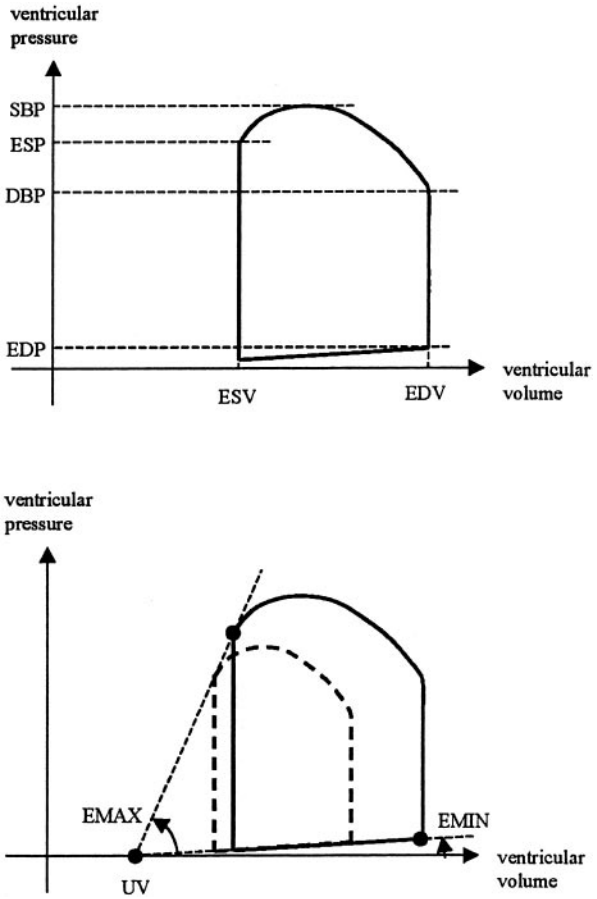

Figure 4. Ventricular pressure-volume curve. A, Clinical variables: end-systolic volume (ESV), end-diastolic volume (EDV), and end-systolic and end-diastolic pressures (ESP and EDP). B, Model parameters: minimum and maximum elastances (EMIN and EMAX) and unstressed volume. The dashed curve represents a situation with identical parameters but reduced preload. SBP = systolic blood pressure; DBP = diastolic blood pressure; UV = unstressed volume.

atrium systole. The ventricle systole starts at time $T_{as} + T_{av}$ after the initiation of the atrium systole, where T_{av} represents the atrioventricular delay.

Beneken gives the duration of atrium and ventricle systole as a function of heart period (HP) and a numerical value for the atrioventricular delay (in seconds):

$$T_{as} = 0.03 + 0.09\text{HP}$$

$$T_{av} = 0.01 \qquad \text{(A10)}$$

$$T_{vs} = 0.16 + 0.20\text{HP}$$

The resistances and unstressed volumes of selected compartments depend on the baroreflex. The baroreflex also affects heart rate and contractility (maximum heart chamber elastance).

The single receptor of the Wesseling and Settels model for the baroreflex (8) is represented by a sigmoid function of mean arterial blood pressure, with a threshold of 50 mm Hg, saturation of 180 mm Hg, and maximum sensitivity around the "resting pressure" of 100 mm Hg. The baroreflex part of the model has four effector variables: heart rate, contractility, total peripheral resistance (TPR), and venous unstressed volume. Parameter data for response gain, delay, and time constant are presented by Ten Voorde (15).

For our study, we implemented a variant of this model. To facilitate parameter estimation and manipulation, we replaced the receptor function with a piecewise linear function with a slope of 1 at the mean arterial blood pressure in equilibrium. The slope is dimensionless, resulting in an output of the receptor function in millimeters of mercury. We maintained the four effector variables, substituting heart period for heart rate. Because our objective was to obtain a realistic simulated response to phenomena such as blood loss and pharmacologic interventions, but not to study beat-to-beat heart rate variability, we maintained the gains but did not include delays or the time constants of the response. Table 4 gives the numerical values for the adult for the baseline baroreflex effectors from Beneken (6), the absolute baroreflex gains of the Wesseling and Settels model in the units specified by Ten Voorde (15), and, for later reference, the derived relative gains in percentage per millimeter of mercury.

In our model, the relative gain for the maximum elastance of the left ventricle is applied to the output of the receptor function, thus affecting the maximum elastance of all four heart chambers. The baroreflex-mediated change in the RSP (resistance of the systemic peripheral vessels) parameter of the Beneken model (Table 3) is such that the total peripheral resistance change is equal to the relative gain. The relative gain for the (total) unstressed volume affects the unstressed volumes of both intrathoracic and extrathoracic compartments.

Appendix 2: Parameter Estimation for Infant Cardiovascular Physiology

The following provides explicit documentation of the steps taken for derivation of specific model parameters for the infant.

Left Heart

From the clinical variables describing the left ventricle (Table 2), assuming a left ventricular unstressed volume of 2.0 mL and an average intrathoracic pressure of −3.25 mm Hg (16), the model parameters for the left ventricle diastolic and maximum systolic elastances were derived by using Equations A7 and A8. The

Table 4. Numerical Values for the Adult Baroreflex Effectors and Gains

Baroreflex effector	Baseline value	Absolute gain	Relative gain
Heart period	833 ms	16.6 ms/mm Hg	1.99% /mm Hg
Maximum elastance of the left ventricle	4.00 mm Hg/mL	−0.0160/mL	−0.40%/mm Hg
Total peripheral resistance	1.15 mm Hg · mL^{-s}	−0.0270 s/mL	−2.35%/mm Hg
Venous unstressed volume	2190 mL	27.0 mL/mm Hg	1.23%/mm Hg

assumed and calculated parameter values are listed in Table 3. Aortic valve resistance, mitral valve resistance, and left atrial inflow tract resistance were each doubled with respect to the adult values. Left atrial unstressed volume was decreased proportionally from the adult value by comparison to the left ventricle. The left atrial minimum and maximum elastances were proportionally increased from adult values by comparison to the left ventricle, because no data concerning the infant atria were available.

Systemic Circulation

Systemic vascular resistance was a calculated value and for an infant was equal to 10–20 mm Hg · L^{-1} · min · m^2 (17). This value is a function of body-surface area and was similar in infants and adults (18). Because of the infant's smaller body-surface area, its absolute value for systemic vascular resistance was approximately twice that of an adult. Accordingly, the infant parameters resistance of the extrathoracic arteries and veins and of the systemic peripheral vessels were obtained by multiplying adult parameters by 2.

The literature provided a value of 0.46 mL/mm Hg for the arterial compliance in infants (19). The adult systemic arterial compliance in the Beneken model is equal to (1/EITHA) + (1/EETHA) = 2.5 mL/mm Hg, where EITHA and EETHA are the elastances of the intrathoracic and extrathoracic arteries, respectively. The ratio between pediatric and adult systemic arterial elastance is therefore equal to 2.5/0.46 ≈ 5.43. Infant EITHA and EETHA were derived by proportionally increasing these values from those of the adult by using this ratio. The same ratio was used to derive the elastance of the intrathoracic and extrathoracic veins.

Arterial and venous unstressed volumes were each proportionally decreased from those of the adult model on the basis of comparison of total blood volumes for that of an infant (80 mL/kg) versus an adult (70 mL/kg) (20). For an 8-kg infant and a 70-kg adult, this leads to a proportionality constant of approximately 0.13. Note that this assumes a similar distribution of blood between arterial and venous circulations in adults and infants.

The above-mentioned parameters were then incorporated in the model software to yield the first iteration of vital signs for the uncontrolled left heart and systemic loop of the infant cardiovascular system. The blood flow inertia parameter was adjusted to optimize the pressure wave form in the intrathoracic artery compartment. Note that when this parameter is used in such an empirical fashion, it should no longer be referred to in terms of underlying physics.

Right Heart

In the infant, the end-diastolic volume (EDV) of the right ventricle is approximately 1.5 times the EDV of the left ventricle (21). We applied this ratio to the unstressed volume going from the left to right ventricle and did the same going from the left to the right atrium. Right atrial and ventricle minimum and maximum elastances were derived by scaling the right heart from adult to infant in the same way as the left heart. As for the left heart, all right heart resistances were multiplied by 2.

Pulmonary Circulation

We used a pulmonary peripheral vascular resistance of 3.7 mm Hg · L^{-1} · min = 0.22 mm Hg · mL^{-1} · s, which is within the published range of 2.5–7.5 mm Hg · L^{-1} · min for pediatric patients (17). This value is two times the adult value in the Beneken model (1.83 mm Hg · L^{-1} · min = 0.11 mm Hg · mL^{-1} · s) and is therefore also consistent with changes made to the systemic circulation. Elastance of the pulmonary arteries and pulmonary veins were both derived by increasing these values from those of the adult, proportional to the increase in systemic arterial elastance. Similarly, pulmonary arterial and pulmonary venous unstressed volumes were both proportionally decreased from that of the adult model on the basis of comparison of total blood volume for an infant versus an adult. Note that with more numerical data on changes in pulmonary vascular tone in infancy, the value of this parameter may change.

The right heart and pulmonary circulation parameters were then incorporated in the model software to yield the first iteration of vital signs for the uncontrolled right heart and pulmonary loop of the infant cardiovascular system. Two parameter changes were made to correct a difference in right and left cardiac output. Table 3 contains the corrected parameters. Subsequently, we combined the two halves of the circulation and simulated the full uncontrolled infant system with the parameters summarized in Table 3. Throughout the simulations, we maintained a constant intrathoracic pressure of −3.25 mm Hg.

Baroreflex

There are no published data for the baroreflex of a 6-mo-old infant. The parameters for the baroreflex were therefore derived from published data concerning the neonate (22). Drouin et al. (22) observed a spontaneous baroreflex sensitivity in full-term neonates of 10.23 ms/mm Hg to changes in systolic blood pressure. At a heart period of 465 ms (heart rate of 129 bpm), this corresponds to a relative baroreflex gain for the heart period of 2.2%/mm Hg. This relative change is similar to that of the adult (Table 4). We used the same relative gains as in the adult for all baroreflex control effectors: heart period, contractility, peripheral resistance, and venous unstressed volume.

J. S. Gravenstein and M. L. Good provided encouraging and guiding comments for this study.

References

1. Good ML, Gravenstein JS. Training for safety in an anesthesia simulator. Semin Anesth 1993;12:235–50.
2. Gaba DM, DeAnda A. The response of anesthesia trainees to simulated critical incidents. Anesth Analg 1989;68:444–51.
3. Howard SK, Gaba DM, Fish KJ, et al. Anesthesia crisis resource management training: teaching anesthesiologists to handle critical incidents. Aviat Space Environ Med 1992;63:763–70.
4. Euliano TY, Caton D, van Meurs W, Good ML. Modeling obstetric cardiovascular physiology on a full-scale patient simulator. J Clin Monit 1997;13:293–7.
5. Halamek LP, Kaegi DM, Gaba DM, et al. Time for a new paradigm in pediatric medical education: teaching neonatal resuscitation in a simulated delivery room environment. Pediatrics 2000;106:E45.
6. Beneken JEW. A mathematical approach to cardiovascular function: the uncontrolled human system [PhD thesis]. Medisch Fysisch Institut TNO, Utrecht, The Netherlands: 1965.
7. Beneken JEW, DeWit B. A physical approach to hemodynamic aspects of the human cardiovascular system. In: Reeve EB, Guyton AC, eds. Physical bases of circulatory transport: regulation and exchange. Philadelphia: Saunders, 1967:1–45.
8. Wesseling KH, Settels JJ. Baromodulation explains short-term blood pressure variability. In: Orlebeke JF, Mulder G, van Doornen LJP, eds. Psychophysiology of cardiovascular control. New York: Plenum Press, 1985:69–97.
9. Van Meurs WL, Good ML, Lampotang S. Functional anatomy of full-scale patient simulators. J Clin Monit 1997;13:317–24.
10. Pruitt AW, Gersony WM. The cardiovascular system. In: Behrman RE, ed. Nelson textbook of pediatrics. 14th ed. Philadelphia: Saunders, 1992:1125–227.
11. Gregory GA. Monitoring during surgery. In: Gregory GA, ed. Pediatric anesthesia. New York: Churchill Livingstone, 1994: 261–79.
12. Graham TP Jr, Jarmakani MM. Evaluation of ventricular function in infants and children. Pediatr Clin North Am 1971;18: 1109–32.
13. Wodey E, Plady P, Copin C, et al. Comparative hemodynamic depression of sevoflurane versus halothane in infants. Anesthesiology 1997;87:795–800.
14. Suga H, Sagawa K, Shoukas AA. Load independence of the instantaneous pressure-volume ratio of the canine left ventricle and effects of epinephrine and heart rate on the ratio. Circ Res 1973;2:314–22.
15. Ten Voorde B. Modeling the baroreflex: a system analysis approach [PhD thesis]. Vakgroep Medische Fysica, Amsterdam, The Netherlands: 1992.
16. Cunningham MD. Bedside pulmonary function testing of infants. In: Levin DL, Morriss FC, eds. Essentials of pediatric intensive care. St. Louis: Quality Medical, 1990:878–83.
17. Strafford MA. Cardiovascular physiology. In: Motoyama EK, Davis PJ, eds. Smith's anesthesia for infants and children. St. Louis: Mosby, 1996:69–104.
18. Lake CL. Cardiovascular anatomy and physiology. In: Barash PG, Cullen BF, Stoelting RK, eds. Clinical anesthesia. Philadelphia: Lippincott, 1992:989–1020.
19. Hsieh K, Chen P, Fu S. A simple, noninvasive method to investigate vascular characteristics in children. Angiology 1996;47: 361–7.
20. Stoelting RK, Miller RD. Basics of anesthesia. Philadelphia: Churchill Livingstone, 2000:364–75.
21. Thilenius OG, Argilla RA. Angiographic right and left ventricular volume determination in normal infants and children. Pediatr Res 1974;8:67–74.
22. Drouin E, Gournay V, Calamel J, et al. Assessment of spontaneous baroreflex sensitivity in neonates. Arch Dis Child Fetal Neonatal Ed 1997;76:F108–12.